The Journal of Immunology

RESEARCH ARTICLE | MARCH 15 2022

Aberrant HO-1/NQO1–Reactive Oxygen Species–ERK Signaling Pathway Contributes to Aggravation of TPA-Induced Irritant Contact Dermatitis in Nrf2-Deficient Mice

Junkai Huang; ... et. al

J Immunol (2022) 208 (6): 1424–1433.
https://doi.org/10.4049/jimmunol.2100577

Aberrant HO-1/NQO1–Reactive Oxygen Species–ERK Signaling Pathway Contributes to Aggravation of TPA-Induced Irritant Contact Dermatitis in Nrf2-Deficient Mice

Junkai Huang,*,†,[1] Xiaoyue Feng,*,†,[1] Jie Zeng,*,†,[1] Shuchang Zhang,*,† Jing Zhang,*,† Pan Guo,*,† Haoyue Yu,*,† Mengke Sun,*,† Jiangmei Wu,*,† Mengyan Li,*,† Yingxi Li,*,† Xiaohua Wang,‡ and Lizhi Hu*,†

NF-erythroid 2–related factor 2 (Nrf2) is a major transcription factor to protect cells against reactive oxygen species (ROS) and reactive toxicants. Meanwhile, Nrf2 can inhibit contact dermatitis through redox-dependent and -independent pathways. However, the underlying mechanisms of how Nrf2 mediates irritant contact dermatitis (ICD) are still unclear. In this article, we elucidated the role of Nrf2 in 12-*O*-tetradecanoylphorbol-13-acetate (TPA)-induced acute ICD. Our study demonstrated that the ear thickness, redness, swelling, and neutrophil infiltration were significantly increased, accompanied by increased expression of inflammatory cytokines (IL-1α, IL-1β, IL-6, etc.) and decreased expression of antioxidant genes (HO-1 and NQO1) in Nrf2 knockout mice. Moreover, ERK phosphorylation was elevated in mouse embryonic fibroblasts (MEFs) from Nrf2 knockout mouse. Inhibition of ERK significantly alleviated TPA-induced cutaneous inflammation and ROS accumulation in MEFs derived from mouse. Conversely, ROS scavenging inhibited the ERK activation and TPA-induced inflammation in MEFs. Taken together, the findings illustrate the key role of the Nrf2/ROS/ERK signaling pathway in TPA-induced acute ICD. ***The Journal of Immunology*****, 2022, 208: 1424–1433.**

Inflammation is an adaptive response to protect organisms from harmful stimuli and injuries. As a redox-sensitive transcription factor, NF-erythroid 2–related factor 2 (Nrf2) not only protects cells against oxidative stress but also plays pivotal roles in attenuating inflammation (1, 2). Recent studies showed that Nrf2 deficiency aggravates inflammation in a variety of disorders, such as colitis, sepsis, and pneumonia in mouse models (3, 4). In lung inflammation models, Nrf2 deficiency aggravates pulmonary inflammation and hyperoxia caused by smoking (5). Several studies have demonstrated that Nrf2 participates in the anti-inflammatory process by orchestrating the recruitment of inflammatory cells and regulating gene expression (6). Thus, Nrf2 is essential to control the inflammatory response. Although the role of Nrf2 in inflammation is complex and not fully understood, a line of evidence suggests that Nrf2 may attenuate inflammation through an antioxidant pathway.

Inflammation and oxidative stress are closely related pathophysiological events. Studies have shown that Nrf2 exhibits an anti-inflammatory property mainly through two pathways: redox-dependent and -independent pathways (7, 8). In the redox-independent pathway, activation of Nrf2 destroys the recruitment of the RNA polymerase II at the IL-6 and IL-1β promoter sites and further attenuates the inflammatory phenotype in macrophages (9, 10). In the redox-dependent pathway, Nrf2 binds to the antioxidant response elements that are located in the promoter region encoding many antioxidant genes, such as NQO1 and HO-1, which play a critical role in cell defense by enhancing the elimination of reactive oxygen-derived species (11–13). However, considering the dynamic of occurrence and development of inflammation, the mechanism of Nrf2 in different inflammation processes still needs to be elucidated.

Contact dermatitis (CD), a common inflammatory disease of the skin, includes irritant CD (ICD) and allergic CD (ACD) (14). ICD is caused by the direct toxic effects of irritants on epidermal keratinocytes, disrupting the skin barrier and triggering the innate immune system, while ACD is a delayed (type 4) hypersensitivity reaction to exogenous exposure to Ag, which is mainly mediated by the interaction of T cells and cytokines (15). In the process of ACD and ICD,

*Immunology Department, Key Laboratory of Immune Microenvironment and Disease (Ministry of Education), Tianjin Medical University, Tianjin, China; †Department of Pathogen Biology and Immunology, Basic Medical College, Tianjin Medical University, Tianjin, China; and ‡Dermatology Hospital, Southern Medical University, Guangzhou, China

[1]J.H., X.F., and J. Zeng contributed equally to this work.

ORCIDs: 0000-0003-0026-9934 (J.H.); 0000-0002-7177-018X (X.F.); 0000-0003-2649-9797 (J. Zeng); 0000-0003-4065-1265 (S.Z.); 0000-0001-7525-2075 (J. Zhang); 0000-0003-3320-3026 (P.G.); 0000-0002-4671-9518 (H.Y.); 0000-0002-2305-2693 (M.S.); 0000-0002-0982-436X (J.W.); 0000-0001-8707-2696 (M.L.); 0000-0002-3848-1992 (Y.L.); 0000-0001-7827-5491 (X.W.); 0000-0002-2933-2207 (L.H.).

Received for publication June 16, 2021. Accepted for publication December 6, 2021.

This work was supported by National Natural Science Foundation of China and Tianjin Medical University (Grants NSFC 81972962, 81573075, and 81301360 to L.H).

J.H., X.F., X.W., and L.H. conceptualized and designed the study. J.H., X.F., J. Zeng, and S.Z. performed the experiments and acquired data. J. Zeng, P.G., H.Y., and M.S. validated the experimental data. J.H., X.F., J.W., M.L., Y.L., and X.W. visualized the data. J.H., X.F., J. Zhang, S.Z., X.W., and L.H. analyzed and interpreted the data. J.H., X.F., J. Zeng, and L.H. drafted the manuscript. All authors approved the final version of the manuscript.

Address correspondence and reprint requests to Prof. Lizhi Hu, Immunology Department, Key Laboratory of Immune Microenvironment and Disease (Ministry of Education), Tianjin Medical University, Tianjin 300070, China. E-mail address: lizhihu@tmu.edu.cn

The online version of this article contains supplemental material.

Abbreviations used in this article: ACD, allergic contact dermatitis; CD, contact dermatitis; ICD, irritant contact dermatitis; KO, knockout; KO-MEF, mouse embryonic fibroblast from Nrf2 knockout; MEF, mouse embryonic fibroblast; MPO, myeloperoxidase; NAC, *N*-acetylcysteine; Nrf2, NF-erythroid 2–related factor 2; OE, overexpression; ROS, reactive oxygen species; TPA, 12-*O*-tetradecanoylphorbol-13-acetate; WT, wild type; WT-MEF, mouse embryonic fibroblast from wild type control.

a series of reactive oxygen species (ROS) are produced (16). Haptens such as DNCB and DNFB can induce contact hypersensitivity, which fully reflects Ag-specific T cell–mediated delayed hypersensitivity (17). The phorbol ester 12-*O*-tetradecanoylphorbol-13-acetate (TPA) is acknowledged as a promoting agent to induce ROS production and ICD (18). Topical application of TPA to the skin leads to the infiltration of inflammatory cells, release and production of proinflammatory cytokines, and production of a large number of ROS. Nrf2 can effectively inhibit inflammation by mediating ROS clearance in acute inflammation of myeloid cells (19). Nrf2 deficiency–induced exacerbation of inflammation is attributable to the overproduction of ROS in LPS-induced mouse sepsis (20). Thus, the antioxidant program modulated by Nrf2 can tightly control the ROS levels in inflammation. In summary, considering that Nrf2 is involved in ACD through oxidative stress, it is reasonable to postulate that Nrf2-mediated ROS clearance may play a pivotal role in alleviation of ICD.

In this study, we used Nrf2-KO (knockout) mice (21) to investigate the role of Nrf2 in the development of ICD and the potential underlying mechanisms. Our data demonstrated that Nrf2 deficiency aggravates TPA-induced ICD mainly through accumulation of ROS. Our findings emphasize the important link between Nrf2 and oxidative stress in inflammatory response.

Materials and Methods

Experimental animals

Nrf2-KO mice on a C57BL/6 background were obtained from Jackson Laboratories. Male mice aged 8 wk old were used in these studies. Sex- and age-matched C57BL/6 mice were from SiPeiFu Company (Beijing, China). All animals were housed in the animal facility of Tianjin Medical University (Tianjin, China). The study was approved by the Institute Research Ethics Committee of Tianjin Medical University.

TPA-induced skin inflammation in mice

Skin inflammation was induced in the ear of 8-wk-old male mice by topical application of 20 μl TPA (P-8139; Sigma) solution (50 μg/ml in acetone). Ear swelling was measured 0, 6, 12, 18, 24, 30, and 36 h after TPA application, and changes in ear thickness were computed as follows: (swelling at each time point) − (swelling at 0 h).

Cell transfection

Mouse embryonic fibroblasts (MEFs) were derived from the dorsal skin of newborn mice. pFLAG-CMV2-mus HO-1 and pFLAG-CMV2-mus NQO1 were transfected, respectively, into MEFs using Lipofectamine 2000 transfection reagent. Real-time RT-PCR was used to assess the expression levels of HO-1/NQO1 mRNA in the MEFs 72 h after transfection. Transfected MEFs were stimulated with TPA (15 nM) for 3 h.

Induction of ACD with DNFB

Induction of ACD with DNFB was performed as described previously (22). Mice were sensitized by a single application of 25 μl DNFB solution (0.4%, v/v dissolved in a 4:1 acetone/olive oil mixture) on the abdomen skin on day 1. On day 6, the mice were challenged with 20 μl DNFB (0.1%, v/v dissolved in a 4:1 acetone/olive oil mixture) on the external aspects of the ear pinnae. The ear thickness was measured using a caliper 0, 6, 12, 18, 24, and 30 h after challenge, and changes in ear thickness were computed as follows: (swelling at each time point) − (swelling at 0 h).

Histological examination

The ear tissue was fixed and embedded in paraffin. The paraffin-embedded specimens were cut into 5- to 7-μm sections and stained with H&E. Neutrophil infiltration into the ear tissue was assessed by measuring myeloperoxidase (MPO) activities, and the infiltrated inflammatory cells were counted. The experimental method of MPO has been detailed in a previous publication (23).

Immunohistochemistry

Serial ear sections 5–7 μm thick were placed on poly-L-lysine–coated slides, deparaffinized in xylene, and rehydrated with a sequence of isopropyl alcohol solutions. Methanol containing 0.3% hydrogen peroxide was used to inactivate endogenous peroxidase at room temperature for 30 min. The nonspecific background was blocked at room temperature using 1% BSA and 5% goat serum in PBS-T (0.1% Tween 80) for 1 h, followed by incubation with the following primary Abs: CD4 (ab183685; Abcam), CD8 (ab209775; Abcam), Nrf2 (ab31163; Abcam), IL-1α (ab7632; Abcam), and IL-1β (ab254360; Abcam) overnight at 4°C. Afterward, slides were washed with PBS-T and incubated with the following secondary Abs: Alexa Fluor 488 (RS3211; Immunoway) and Alexa Fluor 594 (ab150080; Abcam) for 1 h at room temperature. Then DAPI staining of nuclei was followed. Images were photographed using a fluorescence microscope (Carl Zeiss).

Quantitative RT-PCR

Total RNA was isolated using TRIzol reagent (15596018; Life Technologies). cDNA was synthesized with All-in-One First-Strand cDNA Synthesis SuperMix (AE341-02; TransGen Biotech). The real-time RT-PCR was conducted on the 7500 Real Time PCR system, using Green qPCR SuperMix(+Dye II) (AQ602-21; TransGen Biotech). The relative mRNA levels of each sample were determined by the Quote Ct method with the housekeeping gene GAPDH. The primer sequences for real-time RT-PCR are listed in Supplemental Table I.

Western blot analysis

Tissues were homogenized using RIPA Lysis Buffer (CW2333S; CWbio) and 1 mM PMSF (P0100; Solarbio) on ice. The concentration of protein was measured using the Pierce TM BCA Protein Assay Kit (23227; Thermo). Protein bands were separated on 10% SDS-PAGE gels by electrophoresis and the WT and Nrf2-KO samples were on the same gel. Six lanes on the left side were used to load the WT samples and six lanes on the right side were used to load the Nrf2-KO samples. Due to the similar molecular weight, β-Actin expression levels were analyzed on another gel each time when analyzing ERK and p-ERK expression levels. Then, the gels were transferred onto 0.45 μm polyvinylidene-fluoride membranes (IPVH00010; Immobilon). Membranes were blocked with 5% (w/v) nonfat milk in TBST buffer (pH 7.5) for 1 h at room temperature, followed by incubation with the first Ab ERK (9102S; Cell Signaling Technology), p-ERK (4370S; Cell Signaling Technology), and β-Actin polyclonal Ab (YT0099; Immunoway). After washing with TBST for 10 min three times, membranes were incubated with secondary antibodies at room temperature for 1 h. Protein bands were visualized by a chemiluminescence imaging analysis system (Tanon 5200, Shanghai, China) with an ECL reagent (AC 53151; BioWorld). Because simultaneous exposure of two groups of proteins would result in a very faint band for the low expression group and a very intense band for the high expression, we exposed separately for each group and ensured that the ECL luminescent reagent was uniform and the exposure time was consistent for each group, all for 5 s during the exposure process. Further, we quantified the grayscale values of blot through Image J and analyzed the p-ERK/ERK ratios in the WT and Nrf2-KO groups, respectively.

Culture of primary skin fibroblasts

Dermal fibroblasts were derived from the dorsal skin of newborn mice within 24 h after birth and cultured as previously described. Cells were cultured in DMEM (12416001; Corning) supplemented with 10% FBS (AusGeneX, Beijing, China) at 37°C with 5% CO_2 in atmosphere. After treatment with TPA (15 nM) for 3 h, fibroblasts were harvested for the measurement of the expression levels of inflammatory cytokines by real-time RT-PCR.

Measurement of intracellular ROS

Intracellular ROS level was measured by DCFH-DA staining, followed by observation under a fluorescent microscope. All experiment procedures were performed according to the instructions of the Reactive Oxygen Species Assay Kit (CA1410; Solarbio). MEFs grown on a six-well plate were stained with DCFH-DA for 3 h. After washing with PBS, the level of fluorescence, reflecting the concentration of ROS, was measured with a fluorescence microscope, and the final image was captured.

Statistical analysis

Data are expressed as mean ± SD. The unpaired Student *t* test was performed for determination of the significance using Statistical Product and Service Solutions software version 21.0 (SPSS, Chicago, IL).

Results

Nrf2-deficient mice display enhanced inflammatory response in both ICD and ACD

To explore the role of Nrf2 in the development of CD, we assessed the ear thickness, an indicator of ear swelling, in Nrf2-KO versus wild type (WT) mice after topical application of either TPA or

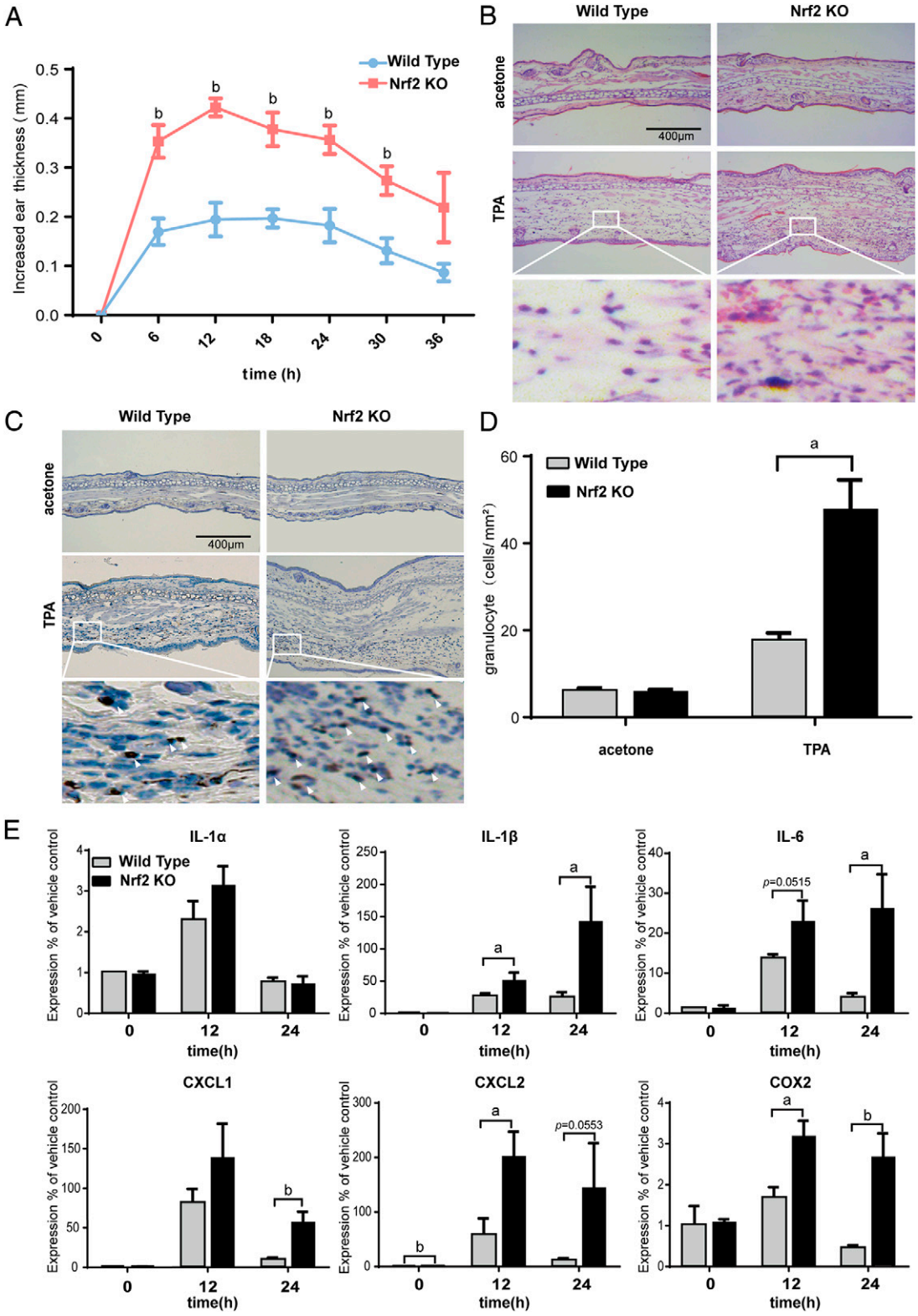

FIGURE 1. Enhanced cutaneous inflammation induced by TPA in Nrf2-KO mice. (**A**) Ear thickness (mm) was measured at 6, 12, 18, 24, 30, and 36 h in Nrf2-KO and WT mice after TPA or acetone application, and increased ear thickness was computed as follows: (swelling at each time point) − (swelling at 0 h). b represents significant differences in ear thickness between Nrf2-KO and WT. (**B**) Representative H&E-stained ear sections; the partially enlarged image highlights the number of infiltrating inflammatory cells. (**C**) MPO activities were measured 24 h after TPA treatment, and the white arrow points to MPO-positive cells. (**D**) Numbers of MPO-positive cells were quantified under ×10 fields. (**E**) mRNA expression was measured by real-time RT-PCR in Nrf2-KO and WT mice 0, 12, and 24 h after TPA or acetone application. $n = 3$ for all. $^{a}p < 0.05$, $^{b}p < 0.01$.

DNFB to the dorsal ear. As shown in Fig. 1, the ear was much thicker in Nrf2-deficient mice than in the WT controls in the ICD model (Fig. 1A, 1B, Supplemental Fig. 1A), accompanied by increased MPO activities (Fig. 1C) and neutrophil infiltration (Fig. 1D). In parallel, the expression levels of mRNA for a panel of cutaneous inflammatory cytokines (IL-1β, IL-6), chemokines

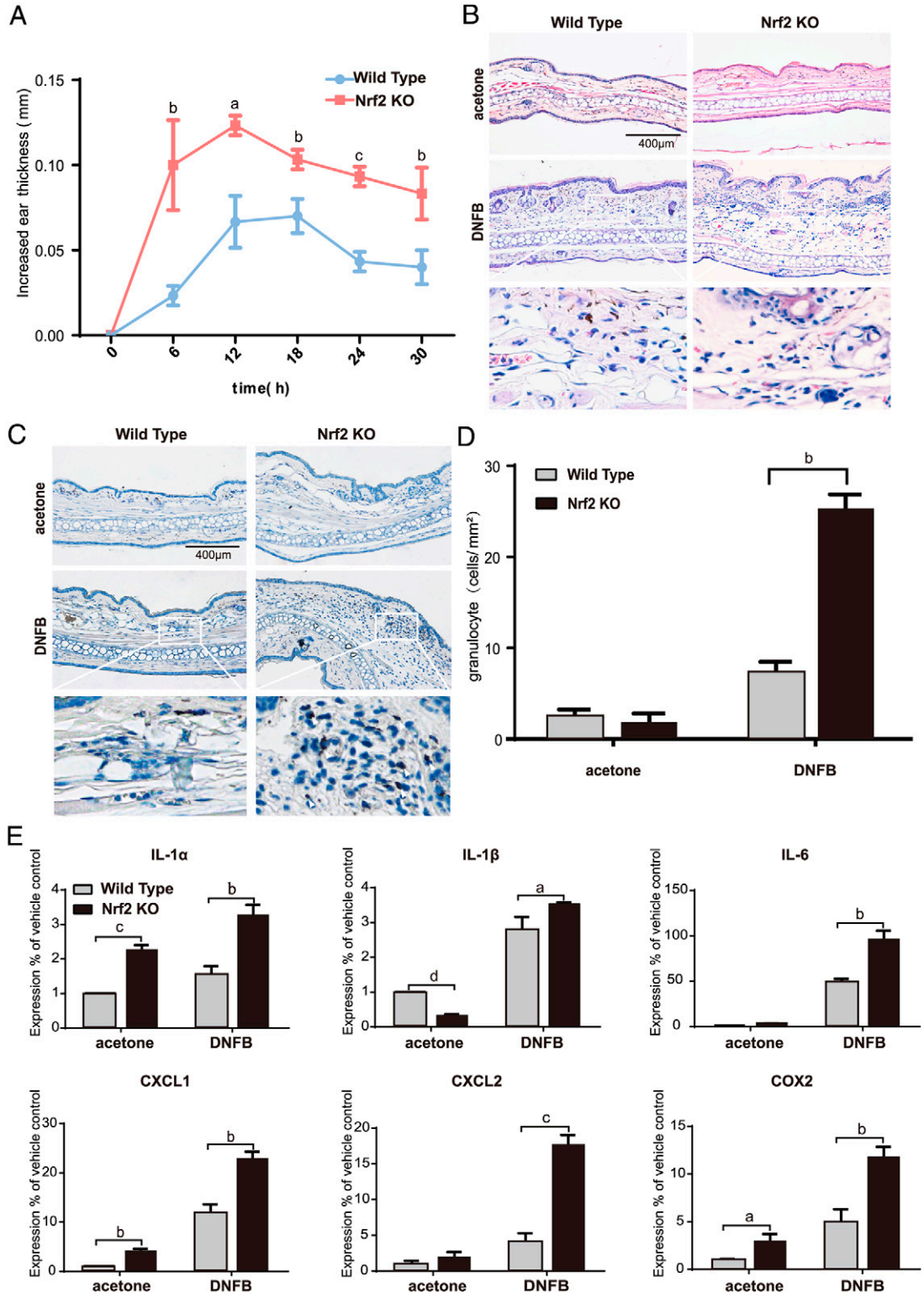

FIGURE 2. Nrf2-KO mice display aggravated cutaneous inflammation induced by DNFB. (**A**) Ear thickness (mm) was measured in Nrf2-KO and WT mice 6, 12, 18, 24, and 30 h after DNFB sensitization, and increased ear thickness was computed as follows: (swelling at each time point) − (swelling at 0 h). a, b, and c represent the significant differences in ear thickness between Nrf2-KO and WT. (**B**) H&E staining of ear sections; the partially enlarged image highlights the number of infiltrating inflammatory cells. (**C**) MPO activities were measured 24 h after DNFB treatment, and the white arrow points to MPO-positive cells. (**D**) Numbers of MPO-positive cells were quantified under ×10 fields. (**E**) The inflammatory cytokine mRNA expression was analyzed by real-time RT-PCR. $n = 3$ for all. $^{a}p < 0.05$, $^{b}p < 0.01$, $^{c}p < 0.001$, $^{d}p < 0.0001$.

(CXCL1, CXCL2), and inflammatory mediator (COX2) were markedly elevated in Nrf2-deficient mice in comparison with the WT controls, while the expression levels of IL-1α were comparable between Nrf2-deficient and WT mice (Fig. 1E). Similar results were obtained in the ACD model (Fig. 2, Supplemental Fig. 1B). To better characterize the ACD model,

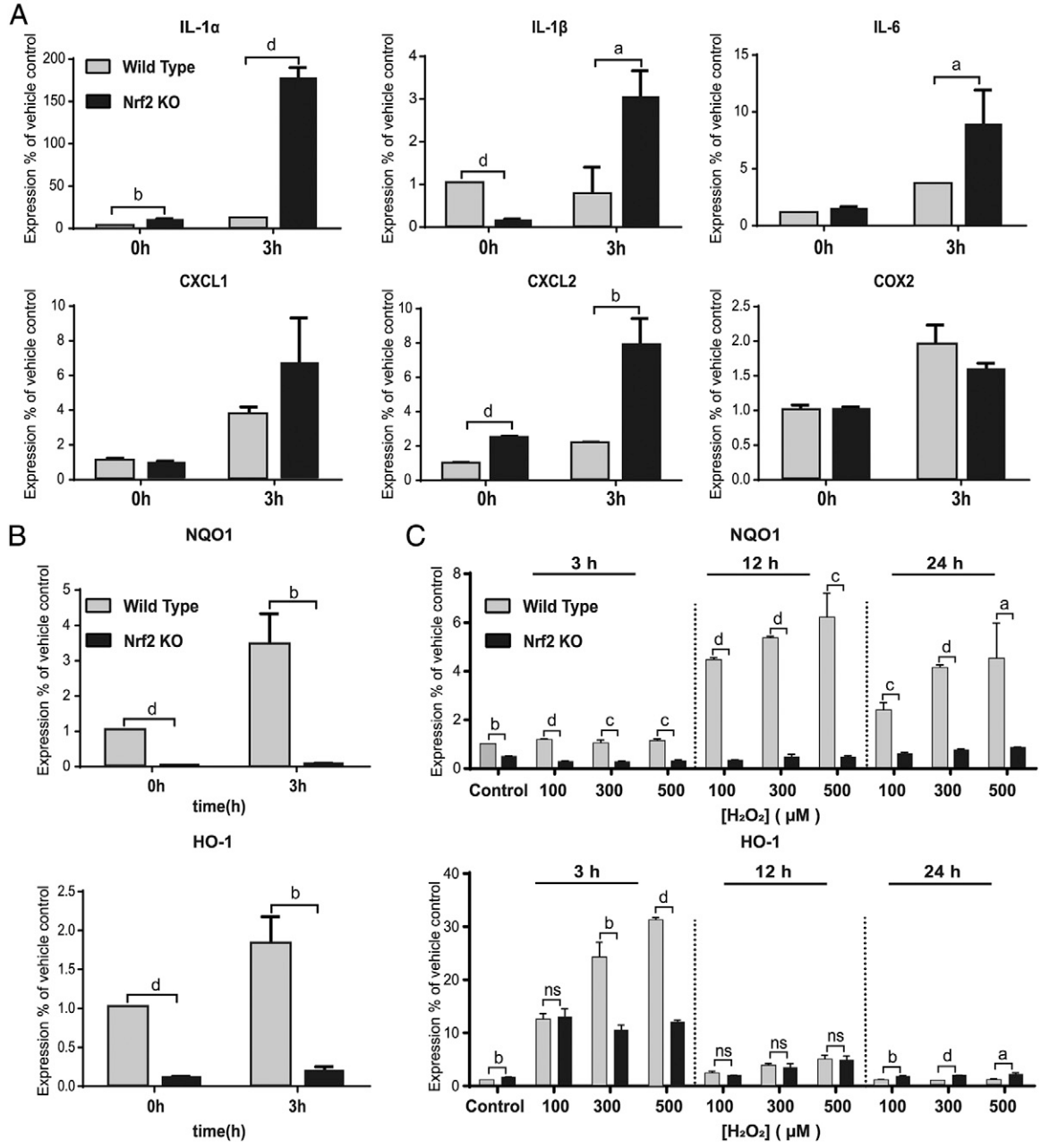

FIGURE 3. TPA increases expression levels of mRNA for inflammatory cytokines HO-1 and NQO1 in fibroblasts. (**A**) Inflammatory cytokine mRNA expression in MEFs from Nrf2-KO and WT mice was measured by real-time RT-PCR 0 and 3 h after TPA treatment. (**B**) mRNA expression of HO-1 and NQO1 in MEFs from Nrf2-KO and WT mice were measured by real-time RT-PCR 0 and 3 h after TPA treatment. (**C**) MEF cells were treated with 100, 300, and 500 μM H_2O_2 for 3, 12, and 24 h. Relative mRNA expression levels of HO-1 and NQO1 were measured by real-time RT-PCR. $n = 3$ for all. $^{a}p < 0.05$, $^{b}p < 0.01$, $^{c}p < 0.001$, $^{d}p < 0.0001$.

we further analyzed T cell infiltration and related cytokine expression. Results showed that $CD4^+$ and $CD8^+$ T cells were recruited to the skin, and Th1/Th2 cytokines were upregulated in both WT and Nrf2-KO mice, but with no significant difference between the two groups (Supplemental Fig. 2A, 2B). These results indicate that Nrf2 deficiency aggravates cutaneous inflammation in both ICD and ACD models.

Nrf2 deficiency–induced oxidative stress contributes to enhanced inflammation in fibroblasts

Because Nrf2 regulates antioxidant defense, next we determined whether oxidative stress accounts for the enhanced inflammation in Nrf2-deficient mice. We first localized the inflammation induced by topical TPA application. As shown in Supplemental Fig. 3A, IL-1α and IL-1β expression were primarily localized in the dermis. Therefore, MEFs were used to determine the involvement of oxidative stress in TPA-induced inflammation. After incubation with 15 nM TPA for 3 h, expression levels of mRNA for IL-1α, IL-1β, IL-6, and CXCL2 were significantly increased in MEFs from Nrf2-KO (KO-MEFs) in comparison with that from WT controls (WT-MEFs) (Fig. 3A). Because both HO-1 and NQO1 are downstream genes of Nrf2, we also measured the expression levels of HO-1 and NQO1 in MEF after TPA treatment. As shown in Fig. 3B, TPA treatment significantly increased expression levels of mRNA for both HO-1 and NQO1 in WT-MEFs, but not in KO-MEFs. Similarly, treatment with H_2O_2 increased HO-1 and NQO1 in WT-MEFs, but not in KO-MEFs (Fig. 3C).

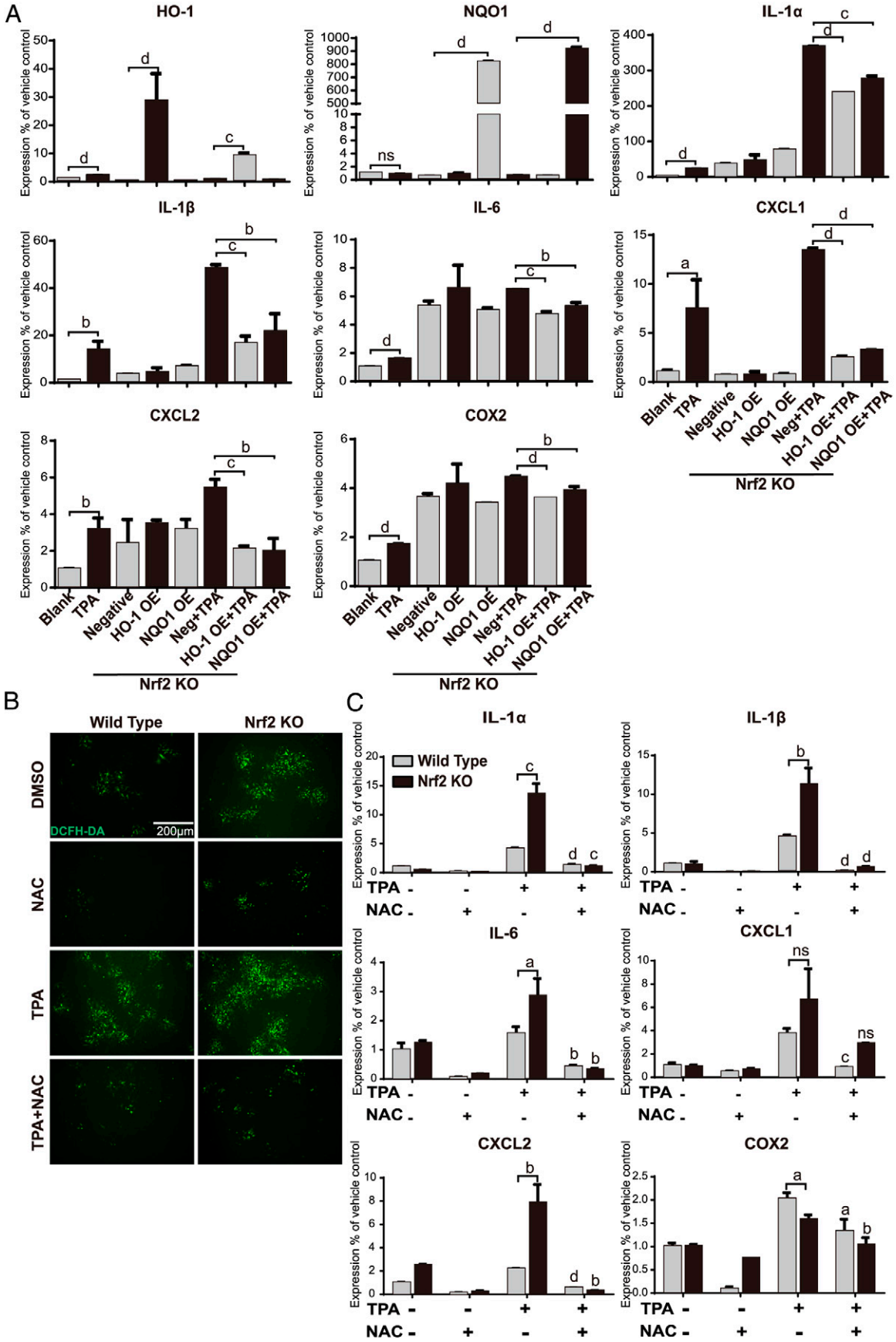

FIGURE 4. Restoration of antioxidant capacity can alleviate inflammation exacerbated by Nrf2 deficiency. (**A**) pFLAG-CMV2-mus HO-1 and pFLAG-CMV2-mus NQO1 were transfected into MEFs, respectively, and then stimulated with TPA (15 nM) for 3 h. The inflammatory cytokine mRNA expression was analyzed by real-time RT-PCR. (**B**) MEF cells were pretreated with ROS inhibitor, NAC (1 mM), for 1 h and then treated with 15 nM TPA for 3 h. ROS level was measured by DCFH-DA assay under a fluorescence microscope. (**C**) Inflammatory cytokine mRNA expression was measured by real-time RT-PCR 0 and 3 h after TPA stimulation. $n = 3$ for all. $^{a}p < 0.05$, $^{b}p < 0.01$, $^{c}p < 0.001$, $^{d}p < 0.0001$.

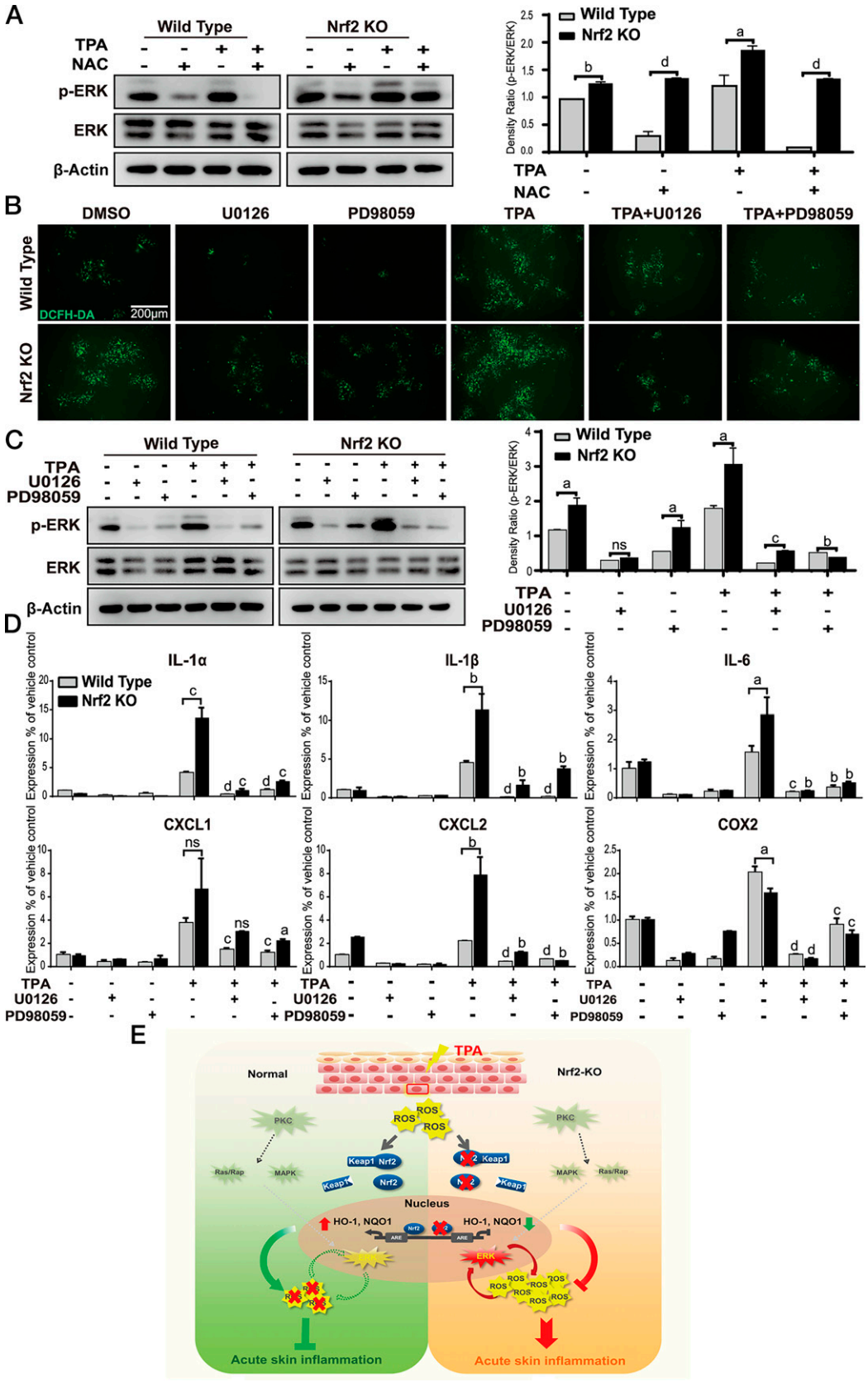

FIGURE 5. Nrf2 mediates TPA-induced inflammation through the ROS–ERK pathway. (**A**) MEF cells were pretreated with ROS inhibitor, NAC (1 mM), for 1 h, and then treated with 15 nM TPA for 3 h. Relative expression levels of ERK and p-ERK protein were determined using Western blotting. β-Actin samples were run on separate gels, and WT and Nrf2-KO groups of proteins were exposed, respectively. Each β-Actin/ERK/p-ERK blot was from the same sample and the loading volume was consistent. Grayscale values of p-ERK/ERK ratios in the WT and Nrf2-KO groups were quantified by ImageJ. (**B**) MEF cells were pretreated with U0126 (10 μM) and PD98059 (10 μM) for 1 h and then treated with 15 nM TPA for 3 h. ROS level was measured by DCFH-DA assay under a fluorescence microscope. (**C**) Relative expression levels of ERK and p-ERK protein were determined using Western blotting. β-Actin samples were run on separate gels, and WT and Nrf2-KO groups of proteins were exposed, respectively. Each β-Actin/ERK/p-ERK blot was from the *(Figure legend continues)*

To determine whether Nrf2 deficiency–induced enhancement of inflammation is attributable to the diminished HO-1 and NQO1 expression, we transfected KO-MEFs with HO-1 and NQO1 plasmids, followed by stimulation with TPA. The expression levels of HO-1 and NQO1 were significantly increased in KO-MEFs 72 h after transfection. Overexpression of either HO-1 or NQO1 largely prevented the elevation of IL-1α, IL-1β, IL-6, CXCL1/2, and COX2 expression in KO-MEFs after TPA treatment (Fig. 4A). It is well known that both HO-1 and NQO1 exert antioxidant properties through scavenging ROS. To ascertain that the prevention of inflammation is due to antioxidation in HO-1– and NQO1-overexpressed KO-MEFs, we measured expression levels of proinflammatory cytokines in KO-MEFs treated with *N*-acetylcysteine (NAC), an intracellular ROS scavenger. TPA treatment dramatically increased ROS in KO-MEFs, while NAC treatment almost completely diminished ROS in TPA-treated KO-MEFs (Fig. 4B). In parallel, NAC prevented the increased expression levels of mRNA for proinflammatory cytokines and chemokines in TPA-treated KO-MEFs (Fig. 4C). These results indicate that Nrf2 deficiency results in diminished HO-1 and NQO1, leading to enhanced inflammatory response.

Aberrant ROS–ERK signaling pathway accounts for enhanced inflammatory response in Nrf2-deficient mice

Because MAPK signaling, especially the ERK pathway, is associated with ROS (24), we assessed whether the aberrant ERK signaling pathway contributes to the enhanced inflammatory response in Nrf2-deficient mice. We first assessed expression levels of ERK in KO-MEFs with or without TPA treatment. Our results showed that expression level of p-ERK was higher in KO-MEFs than in WT-MEFs either under basal condition or after TPA treatment (Fig. 5A), whereas scavenger of ROS with NAC significantly downregulated expression level of p-ERK (Fig. 5A). To further determine the role of ERK in ROS-induced inflammation, we used two structurally unrelated ERK inhibitors, U0126 and PD98059, to inhibit ERK activity. As expected, inhibition of ERK decreased both ROS level (Fig. 5B) and p-ERK (Fig. 5C) in MEFs with or without TPA treatment. Moreover, ERK inhibitors also remarkably reduced expression levels of mRNA for proinflammatory cytokines and chemokines (Fig. 5D). Taken together, these results demonstrate that the aberrant HO-1/NQO1–ROS–ERK pathway accounts for the enhanced inflammatory response in Nrf2-deficient mice.

Discussion

Although the role of Nrf2 in anti-inflammation has been demonstrated in various experiments, the underlying mechanisms of how Nrf2 mediates acute inflammation remain unclear. This study demonstrated that Nrf2 deletion aggravates TPA-induced inflammation, accompanied by a significant increase in inflammatory cytokines. Loss of Nrf2 disrupts the redox balance, leading to the accumulation of ROS, consequently activating the ERK pathway and increasing the immune sensitivity to external stimulation. These results suggest a crucial role of Nrf2 in the maintenance of redox equilibrium and the link between oxidative stress and cutaneous inflammation, at least TPA-induced inflammation.

The development of ICD is associated with the release of ROS at an inflamed site. Nrf2 exerts potent cytoprotective effects through antioxidative stress and anti-inflammatory pathways. We showed in this study that Nrf2 deletion exacerbates TPA-induced ICD. TPA stimulation activates protein kinase C and produces an excessive amount of ROS (25). Protein kinase C directly phosphorylates Nrf2 to trigger its nuclear translocation and enhance the ability to resist oxidative stress (26). To clarify whether TPA stimulation can activate Nrf2 via an oxidative stress pathway, we directly stimulated MEFs with H_2O_2 in vitro. The results showed that the expression levels of HO-1 and NQO1 were upregulated after TPA stimulation, indicating that Nrf2 could be activated by ROS generated by TPA stimulation. Nrf2 exerts antioxidant function by inducing its target antioxidant genes, such as HO-1 and NQO1 (27), and loss of them will weaken ROS scavenging ability in Nrf2-deficient MEFs. In NQO1-deficient mice, dendritic epidermal T cells are sensitive to oxidative stress–induced cell death and exacerbate ICD (28), suggesting that HO-1/NQO1 has an anti-inflammatory effect in ICD. We further overexpressed HO-1 and NQO1 in MEFs to verify the inhibitory effect of Nrf2 on TPA-induced ICD through the HO-1/NQO1 pathway. Considering that the intensity of the ACD reaction is correlated to that of the ICD response (29), the orderly performance of Nrf2-mediated antioxidant function in ICD is also crucial to the development of ACD.

Transcription factor Nrf2 has been described to play a protective role in ACD (30). This study demonstrated that Nrf2 deficiency leads to an increased inflammatory response during the elicitation phase, consistent with previous results (30). However, NQO1 deficiency augments croton oil–mediated ear swelling, but it does not affect ear swelling and inflammation induced by DNFB, suggesting a compensatory mechanism between the Nrf2 target genes, HO-1 and NQO1. In our in vitro experiments, we also found that an H_2O_2-induced increase in HO-1 occurred within 3 h, while elevations in NQO1 were observed for up to 24 h. Whether such differences in response time to H_2O_2 can explain the functional compensation of HO-1 and NQO1 remains to be further explored. So far, many studies have confirmed the antioxidative stress effect of Nrf2 in ACD. The skin infiltration of polymorphonuclear is highly dependent on oxidative stress regulated by Nrf2 in the sensitization phase of ACD (31). Nrf2 deficiency and the concomitant higher ROS level lead to hyaluronic acid breakdown in the extracellular matrix, promoting the migration of dendritic cells, and at the same time increasing the basic activation level of natural immune cells (30, 32). This study showed the accumulated ROS and increased expression of CXCL1/2 in Nrf2-deficient MEFs, which might facilitate hyaluronic acid breakdown and dendritic cell migration. Collectively, Nrf2 mediates ACD, at least in part, through the antioxidant pathway. Besides, Nrf2 activation promotes $CD4^+$ T cells toward Th2 differentiation (33), suggesting that Nrf2 may also play a role in the elicitation phase through regulating Treg function. However, we found that there were no significant differences for T cell infiltration and Th1/Th2 cytokines in Nrf2-KO mice versus WT in ACD, indicating that the aggravated cutaneous inflammation in Nrf2-KO mice was specific to the innate myeloid infiltration and the increased inflammatory-related cytokine and chemokine expression, but with no marked effects on the adaptive T cell response.

Experimental studies have evidenced that the anti-inflammatory role of Nrf2 is attributed to interaction between Nrf2 and many

same sample and the loading volume was consistent. Grayscale values of p-ERK/ERK ratios in the WT and Nrf2-KO groups were quantified by ImageJ, respectively. (**D**) Inflammatory cytokine mRNA expression was measured by real-time RT-PCR 0 and 3 h after TPA stimulation. (**E**) TPA induces accumulation of ROS in skin fibroblasts. The deficiency in Nrf2 abolishes the downstream antioxidant gene expression and aberrant antioxidant defense failing to inhibit TPA-induced oxidative stress. This may eventually result in enhanced inflammation. $n = 3$ for all. $^{a}p < 0.05$, $^{b}p < 0.01$, $^{c}p < 0.001$, $^{d}p < 0.0001$.

redox-sensitive inflammatory pathways, including the most studied one, the NF-κB signaling pathway (17). However, in this study, we found that Nrf2 could play an anti-inflammatory role through indirect regulation of the ERK pathway because ERK1/2 was phosphorylated in physiological conditions and TPA stimulation further promoted ERK activation in Nrf2-KO mice, indicating the accumulation of ROS under physiological conditions. Consistent with the previous study, the physiological concentrations of H_2O_2 activate ERK (24), and the deletion of Nrf2 can lead to ROS accumulation in Nrf2-KO brain hippocampal glioneuronal cells (34). In addition, antioxidants can inhibit ERK activity of HeLa cells, and hydrogen peroxide treatment increases phosphorylation of ERK (35). The role of ROS and ERK activation in Nrf2-mediated inflammation response was further demonstrated by inhibition of ERK activity and ROS scavenger. Either inhibition of ERK or ROS scavenger lowered the expression levels of IL-1α, IL-1β, and IL-6 and ROS accumulation in TPA-treated MEFs, indicating the role of the Nrf2–ROS–ERK pathway in regulation of inflammation induced by TPA.

Under normal conditions, both ERK1 (p44) and ERK2 (p42) were phosphorylated within 10 min after TPA treatment (36), consistent with our observation of ERK phosphorylation within 30 min after TPA treatment (data not shown). However, we found that the phosphorylation of ERK was still higher at 3 h in KO-MEFs pretreated with NAC. Because ROS generation occurs in advance of ROS elimination (37), it is possible that Nrf2 deficiency promotes endogenous ROS production and activates the ERK pathway. Nrf2 and NF-κB signaling pathways interact via multiple mechanisms (17). Given the experimental evidence that IQGAP1 binds to Nrf2 and mediates the MEK–ERK signaling pathway, and that MEK–ERK activates Nrf2 (38), whether Nrf2 has other regulatory mechanisms on the MEK–ERK pathway remains to be further explored.

In conclusion, we demonstrated that Nrf2 deficiency leads to the aggravation of TPA-induced acute inflammation in the skin. Absence of Nrf2 causes the loss of redox homeostasis, resulting in accumulation of ROS and sustained activation of the ERK pathway, and consequently leading to a low threshold of sensitivity to allergens and external stimuli in Nrf2-KO mice (Fig. 5D). Taken together, this study demonstrates the key role of the Nrf2/ROS/ERK pathway in TPA-induced cutaneous inflammation and emphasizes the important link between Nrf2 and oxidative stress in inflammatory response.

Acknowledgments

We thank Jing Luo and Qianyu Zhu (Department of Pathogen Biology and Immunology) for significant contributions to this article.

Disclosures

The authors have no financial conflicts of interest.

References

1. Li, W., T. O. Khor, C. Xu, G. Shen, W. S. Jeong, S. Yu, and A. N. Kong. 2008. Activation of Nrf2-antioxidant signaling attenuates NFkappaB-inflammatory response and elicits apoptosis. *Biochem. Pharmacol.* 76: 1485–1489.
2. Müller, M., A. Banning, R. Brigelius-Flohé, and A. Kipp. 2010. Nrf2 target genes are induced under marginal selenium-deficiency. *Genes Nutr.* 5: 297–307.
3. Khor, T. O., M. T. Huang, K. H. Kwon, J. Y. Chan, B. S. Reddy, and A. N. Kong. 2006. Nrf2-deficient mice have an increased susceptibility to dextran sulfate sodium-induced colitis. *Cancer Res.* 66: 11580–11584.
4. Ishii, Y., K. Itoh, Y. Morishima, T. Kimura, T. Kiwamoto, T. Iizuka, A. E. Hegab, T. Hosoya, A. Nomura, T. Sakamoto, et al. 2005. Transcription factor Nrf2 plays a pivotal role in protection against elastase-induced pulmonary inflammation and emphysema. *J. Immunol.* 175: 6968–6975.
5. Iizuka, T., Y. Ishii, K. Itoh, T. Kiwamoto, T. Kimura, Y. Matsuno, Y. Morishima, A. E. Hegab, S. Homma, A. Nomura, et al. 2005. Nrf2-deficient mice are highly susceptible to cigarette smoke-induced emphysema. *Genes Cells* 10: 1113–1125.
6. Kim, J., Y. N. Cha, and Y. J. Surh. 2010. A protective role of nuclear factor-erythroid 2-related factor-2 (Nrf2) in inflammatory disorders. *Mutat. Res.* 690: 12–23.
7. Itoh, K., T. Chiba, S. Takahashi, T. Ishii, K. Igarashi, Y. Katoh, T. Oyake, N. Hayashi, K. Satoh, I. Hatayama, et al. 1997. An Nrf2/small Maf heterodimer mediates the induction of phase II detoxifying enzyme genes through antioxidant response elements. *Biochem. Biophys. Res. Commun.* 236: 313–322.
8. Jian, Z., K. Li, P. Song, G. Zhu, L. Zhu, T. Cui, B. Liu, L. Tang, X. Wang, G. Wang, et al. 2014. Impaired activation of the Nrf2-ARE signaling pathway undermines H2O2-induced oxidative stress response: a possible mechanism for melanocyte degeneration in vitiligo. *J. Invest. Dermatol.* 134: 2221–2230.
9. Taguchi, K., H. Motohashi, and M. Yamamoto. 2011. Molecular mechanisms of the Keap1–Nrf2 pathway in stress response and cancer evolution. *Genes Cells* 16: 123–140.
10. Kobayashi, E. H., T. Suzuki, R. Funayama, T. Nagashima, M. Hayashi, H. Sekine, N. Tanaka, T. Moriguchi, H. Motohashi, K. Nakayama, and M. Yamamoto. 2016. Nrf2 suppresses macrophage inflammatory response by blocking proinflammatory cytokine transcription. *Nat. Commun.* 7: 11624.
11. Lee, J. M., and J. A. Johnson. 2004. An important role of Nrf2-ARE pathway in the cellular defense mechanism. *J. Biochem. Mol. Biol.* 37: 139–143.
12. Ishii, T., K. Itoh, S. Takahashi, H. Sato, T. Yanagawa, Y. Katoh, S. Bannai, and M. Yamamoto. 2000. Transcription factor Nrf2 coordinately regulates a group of oxidative stress-inducible genes in macrophages. *J. Biol. Chem.* 275: 16023–16029.
13. Kwak, M. K., N. Wakabayashi, K. Itoh, H. Motohashi, M. Yamamoto, and T. W. Kensler. 2003. Modulation of gene expression by cancer chemopreventive dithiolethiones through the Keap1-Nrf2 pathway. Identification of novel gene clusters for cell survival. *J. Biol. Chem.* 278: 8135–8145.
14. You, B. R., J. M. Yoo, S. Y. Baek, and M. R. Kim. 2019. Anti-inflammatory effect of aged black garlic on 12-*O*-tetradecanoylphorbol-13-acetate-induced dermatitis in mice. *Nutr. Res. Pract.* 13: 189–195.
15. Novak-Bilić, G., M. Vučić, I. Japundžić, J. Meštrović-Štefekov, S. Stanić-Duktaj, and L. Lugović-Mihić. 2018. Irritant and allergic contact dermatitis—skin lesion characteristics. *Acta Clin. Croat.* 57: 713–720.
16. Kaur, S., M. Zilmer, M. Eisen, T. Kullisaar, A. Rehema, and T. Vihalemm. 2001. Patients with allergic and irritant contact dermatitis are characterized by striking change of iron and oxidized glutathione status in nonlesional area of the skin. *J. Invest. Dermatol.* 116: 886–890.
17. Helou, D. G., S. F. Martin, M. Pallardy, S. Chollet-Martin, and S. Kerdine-Römer. 2019. Nrf2 involvement in chemical-induced skin innate immunity. *Front. Immunol.* 10: 1004.
18. Germolec, D. R., K. A. Shipkowski, R. P. Frawley, and E. Evans. 2018. Markers of inflammation. *Methods Mol. Biol.* 1803: 57–79.
19. Kobayashi, E., T. Suzuki, and M. Yamamoto. 2013. Roles nrf2 plays in myeloid cells and related disorders. *Oxid. Med. Cell. Longev.* 2013: 529219.
20. Thimmulappa, R. K., H. Lee, T. Rangasamy, S. P. Reddy, M. Yamamoto, T. W. Kensler, and S. Biswal. 2006. Nrf2 is a critical regulator of the innate immune response and survival during experimental sepsis. *J. Clin. Invest.* 116: 984–995.
21. Chan, K., R. Lu, J. C. Chang, and Y. W. Kan. 1996. NRF2, a member of the NFE2 family of transcription factors, is not essential for murine erythropoiesis, growth, and development. *Proc. Natl. Acad. Sci. USA* 93: 13943–13948.
22. Sasso, O., M. Summa, A. Armirotti, S. Pontis, C. De Mei, and D. Piomelli. 2018. The N-acylethanolamine acid amidase inhibitor ARN077 suppresses inflammation and pruritus in a mouse model of allergic dermatitis. *J. Invest. Dermatol.* 138: 562–569.
23. Bradley, P. P., D. A. Priebat, R. D. Christensen, and G. Rothstein. 1982. Measurement of cutaneous inflammation: estimation of neutrophil content with an enzyme marker. *J. Invest. Dermatol.* 78: 206–209.
24. Preston, T. J., W. J. Muller, and G. Singh. 2001. Scavenging of extracellular H2O2 by catalase inhibits the proliferation of HER-2/Neu-transformed rat-1 fibroblasts through the induction of a stress response. *J. Biol. Chem.* 276: 9558–9564.
25. Ikuta, S., H. Edamatsu, M. Li, L. Hu, and T. Kataoka. 2008. Crucial role of phospholipase C epsilon in skin inflammation induced by tumor-promoting phorbol ester. *Cancer Res.* 68: 64–72.
26. Huang, H. C., T. Nguyen, and C. B. Pickett. 2000. Regulation of the antioxidant response element by protein kinase C-mediated phosphorylation of NF-E2-related factor 2. [Published erratum appears in 2001 *Proc. Natl. Acad. Sci. USA* 98: 379.] *Proc. Natl. Acad. Sci. USA* 97: 12475–12480.
27. Dinkova-Kostova, A. T., and P. Talalay. 2010. NAD(P)H:quinone acceptor oxidoreductase 1 (NQO1), a multifunctional antioxidant enzyme and exceptionally versatile cytoprotector. *Arch. Biochem. Biophys.* 501: 116–123.
28. Kitajima, M., A. Kimura, and H. Suzuki. 2018. Cutting edge: Nqo1 regulates irritant contact hypersensitivity against croton oil through maintenance of dendritic epidermal T cells. *J. Immunol.* 200: 1555–1559.
29. Bonneville, M., C. Chavagnac, M. Vocanson, A. Rozieres, J. Benetiere, I. Pernet, A. Denis, J.-F. Nicolas, and A. Hennino. 2007. Skin contact irritation conditions the development and severity of allergic contact dermatitis. *J. Invest. Dermatol.* 127: 1430–1435.
30. El Ali, Z., C. Gerbeix, P. Hemon, P. R. Esser, S. F. Martin, M. Pallardy, and S. Kerdine-Römer. 2013. Allergic skin inflammation induced by chemical sensitizers is controlled by the transcription factor Nrf2. *Toxicol. Sci.* 134: 39–48.
31. Helou, D. G., B. Noël, F. Gaudin, H. Groux, Z. El Ali, M. Pallardy, S. Chollet-Martin, and S. Kerdine-Römer. 2019. Cutting edge: Nrf2 regulates

neutrophil recruitment and accumulation in skin during contact hypersensitivity. *J. Immunol.* 202: 2189–2194.
32. Corsini, E., V. Galbiati, D. Nikitovic, and A. M. Tsatsakis. 2013. Role of oxidative stress in chemical allergens induced skin cells activation. *Food Chem. Toxicol.* 61: 74–81.
33. Rockwell, C. E., M. Zhang, P. E. Fields, and C. D. Klaassen. 2012. Th2 skewing by activation of Nrf2 in CD4($^{+}$) T cells. *J. Immunol.* 188: 1630–1637.
34. Kovac, S., P. R. Angelova, K. M. Holmström, Y. Zhang, A. T. Dinkova-Kostova, and A. Y. Abramov. 2015. Nrf2 regulates ROS production by mitochondria and NADPH oxidase. *Biochim. Biophys. Acta* 1850: 794–801.
35. Wang, J., D. Lin, H. Peng, Y. Huang, J. Huang, and J. Gu. 2013. Cancer-derived immunoglobulin G promotes tumor cell growth and proliferation through inducing production of reactive oxygen species. *Cell Death Dis.* 4: e945.
36. Lee, H. W., D. H. Ahn, S. C. Crawley, J. D. Li, J. R. Gum, Jr., C. B. Basbaum, N. Q. Fan, D. E. Szymkowski, S. Y. Han, B. H. Lee, et al. 2002. Phorbol 12-myristate 13-acetate up-regulates the transcription of MUC2 intestinal mucin via Ras, ERK, and NF-kappa B. *J. Biol. Chem.* 277: 32624–32631.
37. Xue, J., C. Yu, W. Sheng, W. Zhu, J. Luo, Q. Zhang, H. Yang, H. Cao, W. Wang, J. Zhou, et al. 2017. The Nrf2/GCH1/BH4 axis ameliorates radiation-induced skin injury by modulating the ROS cascade. *J. Invest. Dermatol.* 137: 2059–2068.
38. Cheung, K. L., J. H. Lee, L. Shu, J. H. Kim, D. B. Sacks, and A. N. Kong. 2013. The Ras GTPase-activating-like protein IQGAP1 mediates Nrf2 protein activation via the mitogen-activated protein kinase/extracellular signal-regulated kinase (ERK) kinase (MEK)-ERK pathway. *J. Biol. Chem.* 288: 22378–22386.